

# Influence of the Stabilising Mechanism and Solid Loading on Slip Casting of Alumina

G. Tari,<sup>a</sup> J. M. F. Ferreira,<sup>a\*</sup> and O. Lyckfeldt<sup>b</sup>

<sup>a</sup>Department of Ceramics and Glass Engineering, University of Aveiro, 3810 Aveiro, Portugal

<sup>b</sup>Swedish Ceramic Institute, Box 5403, S-40229 Goteborg, Sweden

(Received 18 April 1997; accepted 11 August 1997)

## Abstract

Two commercial surface active agents that act through different stabilisation mechanisms, were used to disperse aqueous alumina suspensions. Electrophoretic measurements were performed to determine the zeta potential curves of the bare and surface charge modified alumina particles and, hence, to determine the stabilising performance of the dispersants.

Drying–shrinkage behaviour (Bigot's curves) and Hg porosimetry were used to characterise the slip cast bodies prepared from the suspensions at different solid loading. The rheological behaviour of the starting alumina suspensions was also determined in order to relate the flow properties with the superficial nature of the suspended particles and the wet body microstructure.

Rheological measurements have showed that the slips containing the dispersant that confers the highest zeta potential values to the alumina particles were more viscous than when using the less capable dispersant in terms of surface charge modifier. These findings were explained by a larger interaction size of the particles dispersed through a pure electrostatic mechanism which resulted in a higher effective volume solid fraction of these suspensions.

For both dispersants used, the Bigot's curves indicated that the shrinkage and the slopes of the straight lines corresponding to the first stage of the drying decrease with increasing solids concentration. The variations in the slope derive from a broadening pore size distribution as a result of the increasing difficulties in stabilising the concentrated alumina suspensions, in agreement with the rheological measurements. Good correlations were found between the green microstructure, the rheology of

the suspensions and the particle interaction forces.

© 1998 Elsevier Science Limited. All rights reserved

## 1 Introduction

Ceramic powder suspensions can be considered as colloidal systems when the suspended particles have sizes in the range of 0.1–1  $\mu\text{m}$ .<sup>1</sup> The properties of such colloidal dispersions are dependent on the solid loading, the particle (aggregate) size distribution, the particle (aggregate) shape and the net interaction forces between particles. Because of their size, colloidal particles undergo Brownian motion such that collisions occur between them. The stability and other properties of colloidal dispersions depend on the interplay between interparticle forces, Brownian motion and on whether or not such collisions lead to aggregation. Several types of interactions may occur as two particles approach each other. The origins and mechanisms of different surface forces, and how these forces depend on factors such as the medium between the surfaces has been described in the literature concerned with colloid science,<sup>2,3</sup> direct measurement of specific types of surface forces,<sup>4–7</sup> as well as ceramic processing.<sup>2,8–10</sup> Horn<sup>11</sup> reviewed surface forces and their action within ceramic materials covering the advances that have been made in the last two decades in this field. It seems that the most relevant interactions between oxide particles suspended in aqueous media at low ionic strength, are the attractive van der Waals potential, the electrostatic repulsion resulting from the overlapping of electrical double layers and the steric hindrance resulting from adsorbed molecules of the solvent, surfactants or dispersants present.

In a powder suspension the repulsive forces tend to drive the particles apart, giving a positive contribution to stabilising the suspension.

\*To whom correspondence should be addressed.

Alternatively, attractive forces impart instability to the dispersion leading to aggregate formation and flocculation. The net superposition of all these interactions determines the energy change associated with aggregation and hence the stability. In the absence of the steric contribution, the classic DLVO<sup>12</sup> theory normally provides a good description of the interparticle potentials in ceramic powder dispersions, even if all the surface forces involved in particulate system are not included. This theory assumes that the net force between particles immersed in a polar liquid is given by the algebraic sum of the electrical double layer repulsion and the attractive Van der Waals forces. Hence, the attractive Van der Waals forces are normally balanced by long range repulsive forces that can originate from the natural charging of suspended particle by adjusting the pH, or more frequently, by the surface adsorption of surface active agents, i.e. dispersants. These surface active agents stabilise the ceramic suspension by changing the surface nature and/or the surface charge properties. The effectiveness of the stabilisation depends upon the type of mechanism that generates the repulsive forces between the suspended particles. These repulsive forces usually derive from the interaction between electrical double layers (electrostatic stabilisation) or from the interaction between layers of non charged polymers (steric stabilisation). In some systems, for example with polyelectrolyte type of dispersants, the two mechanisms may be combined (electrosteric stabilisation).

Independently of the stabilising mechanism promoted by the dispersant, the effective volume of one particle (interaction size) is given by its own volume (hard size) plus the range of the interparticle forces. The solid loading of a suspension is calculated from the hard size. However, the effective volume fraction of a dispersed suspension is determined by the interaction size, i.e. the size at which the particles may begin to feel each other's presence.<sup>11</sup> It is well known that the range of electrostatic forces is more extended than steric ones.<sup>13</sup> Hence, the effective volume fraction of the suspended particles is higher than that calculated from the hard size and can be related to the stabilising mechanism. Further, the interacting volumes can be deformed or modified, especially in concentrated suspensions, as following: (i) deformation of the external part of the electrical double layers (diffuse layer), (ii) interaction between electrical double layers of closer particles during motion, and (iii) modification of the conformation of the polyelectrolyte chains adsorbed at the particle surfaces. These effects were classified by Conway *et al.*<sup>14</sup> as primary, secondary and tertiary electroviscous effects, respectively. The influence of

these various electroviscous effects on viscosity was studied by several authors recently reviewed by Diz.<sup>15</sup>

The present work is aimed to study the influence of two dispersants expected to act through different stabilising mechanisms, on the effective volume of suspended alumina particles and on the homogeneity of slip cast microstructures. Dispersed aqueous alumina suspensions were prepared at various solid loading and their rheological properties were correlated to the particle packing ability during slip casting.

## 2 Experimental Procedure

### 2.1 Materials

A commercial alumina powder (A16 SG, Alcoa Chemicals, USA), with a BET specific surface area of  $11 \text{ m}^2 \text{ g}^{-1}$  was used in this study. The dispersants used were a polyacrylic acid (Dolapix CE 64, Hans Barnstorf & C., Germany) that imparts stability by a combination of steric and electrostatic interaction,<sup>16,17</sup> and 4,5 dihydroxy 1,3 benzenedisulfonic acid (Tiron, Aldrich-Chemie, Germany) that acts through pure electrostatic interactions.<sup>18</sup>

### 2.2 Preparation and characterisation of the suspensions

Aqueous alumina suspensions at 30–55 vol% solid loading were prepared using 0.25% Tiron or 0.45% Dolapix (based on alumina), respectively. In an initial study, these optimised amount of dispersants, i.e. that gave slips with the lowest viscosity, were found to be independent on solid loading.

Each slip was prepared by first mixing dispersant and water. Then, while stirring, the powders were added and the resulting suspension was stirred for a further 30 min. Deagglomeration and homogenisation was performed by ball milling in a plastic container for 12 h with  $\text{Al}_2\text{O}_3$  cylindrical grinding media. Subsequently, the slip was conditioned for 6 h, by rolling in the plastic containers without balls in order to stabilise the properties.

The effect of the stabilising mechanism upon the properties of aqueous alumina suspensions was evaluated by electrophoretic and rheological measurements. The electrophoretic analysis was carried out with an instrument (Zetasizer 4, Malvern, UK) that uses a photon-correlation spectroscopy technique. The zeta potential was detected from the motion of particles caused by an external electric field applied to the sample. Measuring the rate of motion (electrophoretic mobility) and using the Smoluchowski<sup>19</sup> equation, the zeta potential of the particles was determined. The analysed suspensions were diluted with an aqueous electrolyte solution

(KCl, 0.001 M) and the pH adjustment was achieved with aqueous solutions of HCl or NaOH. The pH was determined with a pH meter (Corning 240), calibrated with buffer solutions (pH 4, 7 and 10, Merck, Germany).

Rheological measurements were performed with a rotational controlled stress Rheometer (Carri-med 500 CSL, UK), immediately after the slip conditioning at a strictly constant temperature (20°C). The measuring configuration adopted was a concentric coaxial cylinder and both steady shear and stress sweep measurements were conducted between 0.5 and 550 s<sup>-1</sup>. Prior to the measurement, pre-shearing was performed at the highest shear rate value for 1 min, followed by an equilibrium time of 2 min in order to transmit the same rheological history to all the suspensions being tested.

### 2.3 Preparation and characterisation of the green body

The drying-shrinkage behaviour of the green compacts obtained by conventional slip casting from suspensions at different solid loading was determined by using a barelatographe (Adamel Lhomargy, France), a mechanical device that simultaneously measures the variation of weight and length of the sample. Cast bars (length = 110 mm, trapezoidal section with an area of  $[(15 + 17)/2] \times 15 \text{ mm}^2$ ) were obtained by solid casting into suitable plaster moulds and used in the drying experiments. Immediately after demoulding, two specimens of 40 mm were cut, weighed and then carefully placed in the barelatographe for the simultaneous measurements of shrinkage and loss of humidity. The natural drying (at room temperature) of the samples were recorded for one day and following this, the drying was completed in a stove at 120°C for 12 h. The weight and length of the completely dried samples were measured and used as reference for plotting the Bigot's curves. The elaboration of the picture obtained from the barelatographe was performed with an image analyser (Quantimet 500+, version 2.00, Leica). The critical moisture content (CMC) and the slope (dS/dH, where S and H stands for shrinkage and humidity) in the constant-rate period were determined using a linear regression of the data in the first stage of the Bigot's curve.

Finally, the pore size distribution and the density of the slip cast samples were determined by Hg porosimetry (PoreSizer 9320, Micromeritics, USA) and Hg immersion method, respectively. The high pressure part of each Hg porosimetry experiment was carried out using the automatic mode with a equilibration time of 10 s at each point. Before measurement, the samples were completely dried in a stove at 120°C for 24 h.

## 3 Results and discussion

### 3.1 Slip characterisation

The effects of Dolapix and Tiron upon the electrophoretic behaviour of alumina particles are shown in Fig. 1. It can be seen that the addition of dispersants causes significant changes in alumina surface charge properties. The IEP and the curves in their entirety were shifted in the acidic direction in relation to the curve obtained with bare alumina particles. This displacement of the IEP was almost two pH units with Dolapix, and more than three pH units with Tiron. Further, the amplitude of the negative zeta potentials increased in the basic pH region. This effect was more pronounced when Tiron was used, confirming its stronger electrostatic stabilisation action compared to the electrosteric one exerted by Dolapix.<sup>16</sup>

The adsorption of multiple charged ions, such as Tiron, leads to a change in the surface charge which stabilises the suspension mainly by an electrostatic mechanism. For compounds based upon the benzene molecule, Graule and Gauckler<sup>18</sup> concluded that their efficiency as deflocculants was enhanced when two or more hydroxyl groups in ortho-position were used as adsorbing (anchor) groups and when other functional groups were arranged in meta-position, relative to the hydroxyl groups. Figure 2 shows a schematic representation of the adsorption of Tiron onto an alumina surface. This arrangement is favourable, since the repulsive electrostatic interactions between the charging groups is avoided and the alumina surface becomes highly negatively charged. Due of this, Tiron was concluded to be a very effective deflocculant for aqueous alumina suspensions.<sup>18</sup>

Alternatively, for a suspension preparing with high solid volume fraction, it seems reasonable to utilise a dispersant that can adequately stabilise the alumina particles without significantly increasing their effective volume in suspension. The calculated volume fraction corresponds to the solid loading of the slurries and does not take into account the

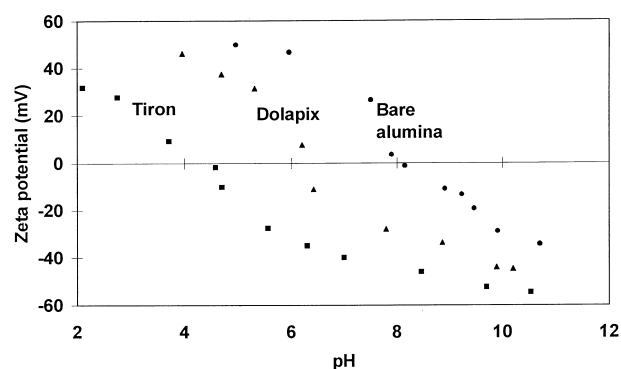


Fig. 1. Effect of dispersants on zeta potential curves for alumina particles.

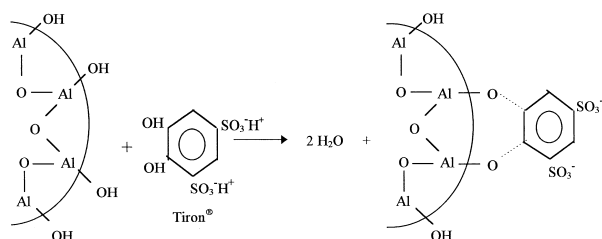


Fig. 2. Model for adsorption of Tiron onto the alumina surface particles.

thickness of the hydrated, adsorbed, or electrical double layers around the alumina particles. However, collisions between particles do not necessarily involve hard-wall contact but could be mediated by interparticle forces, namely electrostatic repulsive forces which are stronger in the presence of Tiron. The interparticle separation at which they may begin to 'feel' each other's presence depends upon the range of surface forces. Thus each particle may be thought of as having an interaction size (effective diameter) which is approximately its diameter plus twice the range of total surface forces (Fig. 3). The distinction between hard size and interaction size becomes important when high solid loading and/or small particles are used. Higashitani *et al.*<sup>20</sup> observed a remarkable decrease in coagulation rate of nearly monodispersed particles in aqueous solution for particle diameters smaller than 85 nm, attributed to a high viscosity layer consisting of water molecules and ions adsorbed onto the particle surface which would be responsible for a shallow primary minimum of the interparticle potential and for a considerable reduction in the colliding velocity of the particles. Further, the viscosity data collected by Ayril *et al.*<sup>21</sup> for aqueous suspensions of silica particles with a mean hard size of  $\approx 17.5$  nm could only be described by the Mooney<sup>22</sup> equation when interaction size was considered. It was found that the viscosity was lower nearer rather than farther away from the IEP of the silica particles. Based upon the viscosity measurements, differences between the hard and the

interaction size were estimated to be approx 4–5 nm in the pH range 9–10, corresponding to high zeta potential values. However, the difference was less than 2 nm at pH 2.

In the alumina slips prepared and stabilised with Tiron and Dolapix the pH was found to be approximately 10. Based upon the difference in the electrostatic potential within this pH range, the interaction size of the particles dispersed with Tiron can be assumed to be larger than with Dolapix. Consequently, the effective volume fraction at a given solid loading should be higher for the suspensions stabilised with Tiron.

Figures 4 and 5 show the viscosity curves and flow curves of the alumina suspensions at various solid concentrations and make it possible to compare the influence of the dispersants upon the rheological behaviour. First, the viscosity of the slips dispersed with Tiron, for a given solid loading, is generally higher than with Dolapix. Further, considering the log scaling, this difference tends to increase with increasing solid loading, confirming the hypothesis regarding the higher effective volume fraction of the alumina particles in the case of Tiron. By its lower electrostatic contribution to stabilisation, Dolapix confers a smaller interaction size to the alumina particles and, hence, a lower viscosity level at a certain solid loading. The lower viscosity also indicates that Dolapix gives a steric contribution to the stabilisation preventing direct contact between particles.

The effect of the solid contents can also be expressed by the rheological behaviour of the slips. The increase in yield stress and plastic viscosity by increasing the solid concentration can mainly be attributed to an higher frequency of the collisions between separate particles, which renders them more resistance to flow. Particles are forced to approach each other and overlap their electrical double layers (electroviscous effect).<sup>14</sup> Further, the accentuation of the shear-thinning characteristic also indicates a more complex structure of the

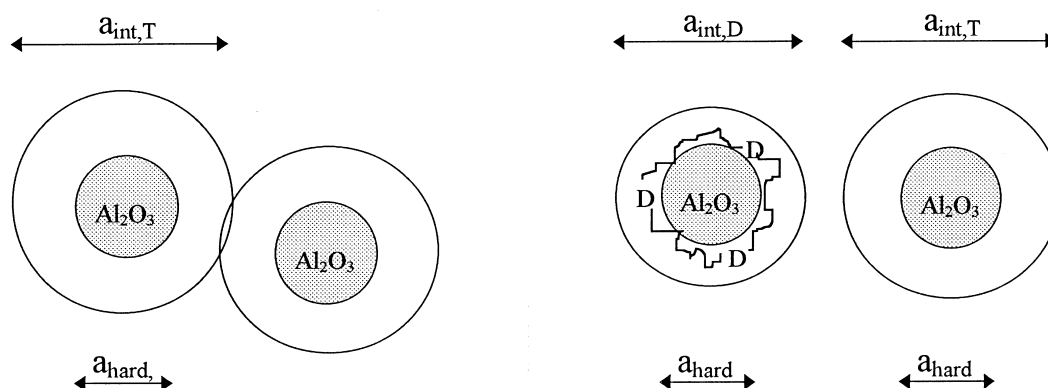


Fig. 3. (a) Hard size ( $a_{\text{hard}}$ ) and interaction size ( $a_{\text{int}}$ ) concept, (b) schematic representation of the interaction size of alumina particles in presence of the two dispersants.

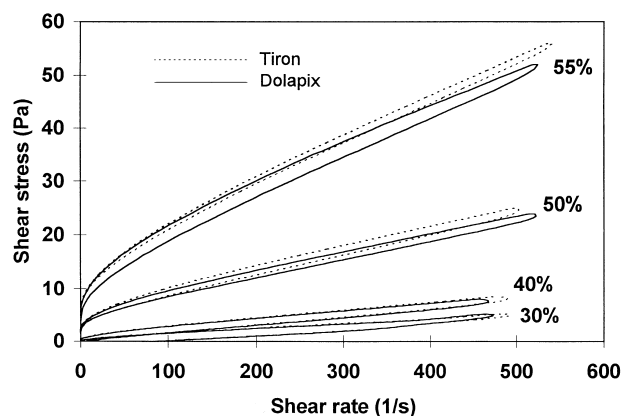


Fig. 4. Flow curves of the alumina suspensions at different solid loading

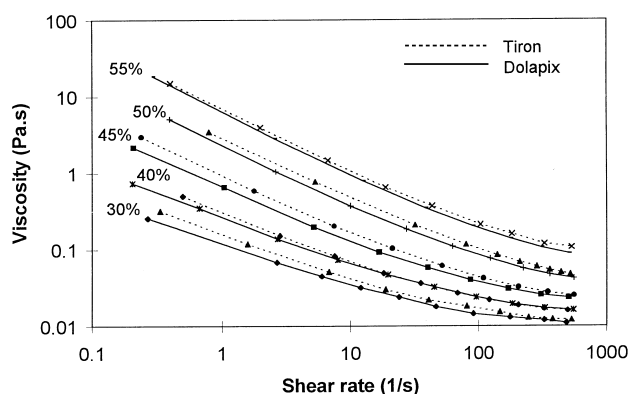


Fig. 5. Effect of solid loading on equilibrium viscosity for suspensions dispersed with Tiron and Dolapix.

suspensions resulting from the increased solid concentration.<sup>24</sup> If particles approach until a distance corresponding to the primary minimum in the total interaction energy, they may coagulate. As a result, a complete stabilisation of the suspensions becomes more difficult. Consequently, the number of flocs will increase, as well as the quantity of entrapped liquid, not available for flow.<sup>23,24</sup>

### 3.2 Green body characterisation

The Bigot's curves of the green bodies prepared from slips at different solid loading and dispersed with Tiron and Dolapix are reported in Fig. 6(a) and (b), respectively. The main features of these curves, and also the density and porosity data are summarised in Table 1.

Figure 6 and Table 1 clearly show a decrease of the linear shrinkage of the slip cast bodies with increasing solid contents, for both dispersants used. These variations are also accompanied by a decrease of the slopes of the straight lines corresponding to the first stage of the drying. The dependence of CMC on solids concentration is qualitatively similar for both dispersants used, showing an initial decrease followed by a trend towards a constant values at higher solid loading.

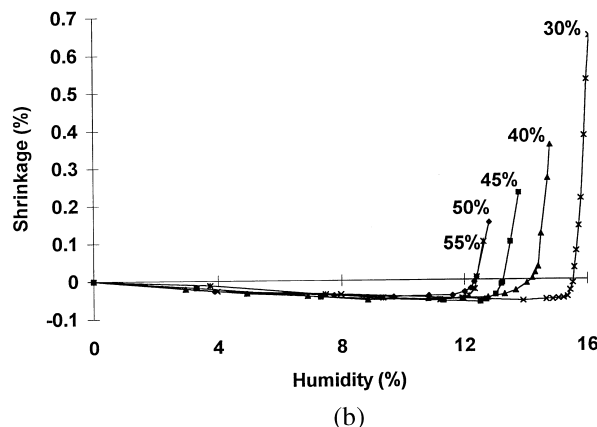
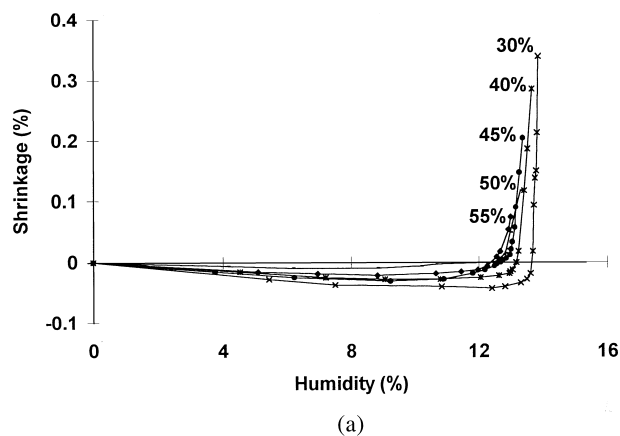


Fig. 6. Bigot's curves of the slip cast bodies obtained from alumina suspensions at different solid contents and dispersed with (a) Tiron and (b) Dolapix.

However, the magnitude of these features of the Bigot's curves (CMC, maximum shrinkage and  $dS/dH$ ), as well as the 'critical' solid content at which the CMC becomes almost constant are quite different for samples prepared with the two dispersants used.

The linear shrinkage is directly connected with the thickness of liquid layers surrounding the particles in the cake, i.e. the amount of free-liquid. An increasing number of particles within suspension sharing the same amount of liquid leads to an higher frequency of mutual collisions and an overlapping of electrical double layers. Hence, a reduction of the hydrated layer around each particle is expected, leading to a closer mutual approach and so, to a higher cast density in the wet state. These results in addition with the previous rheological characterisation of the alumina suspensions show that the microstructure of the slip cast bodies are dependent upon both the solid loading and the type of dispersant. Accordingly, it is possible to distinguish two regimes governing the packing behaviour during slip casting at low and at high solid loading, respectively.

At low solid content, segregation phenomena is likely occur which will lead to gradients and overall

**Table 1.** Drying-shrinkage features, density and porosity of the slip cast bodies obtained from alumina suspensions at different solid loading

	<i>Tiron</i>					<i>Dolapix</i>				
	30	40	45	50	55	30	40	45	50	55
CMC (%)	13.7	13.2	13.0	12.7	12.6	15.6	14.3	13.3	12.4	12.4
Linear shrinkage (%)	0.34	0.29	0.20	0.12	0.08	0.66	0.36	0.23	0.15	0.10
dS/dH	1.51	0.62	0.48	0.21	0.16	1.71	0.69	0.47	0.34	0.42
TD (%)	63.0	64.8	64.6	63.8	64.1	61.6	64.1	65.8	66.0	66.3
Total pore volume (ml g <sup>-1</sup> )	0.127	0.129	0.133	0.136	0.126	0.090	0.124	0.140	0.136	0.122
Mean pore diameter ( $\mu$ m)	0.044	0.045	0.048	0.049	0.044	0.048	0.045	0.048	0.047	0.043

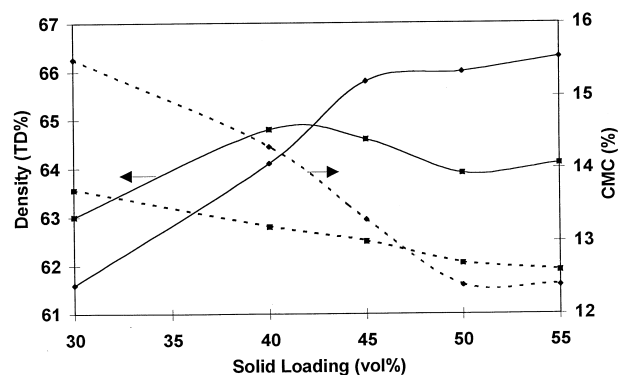
less dense compacts during slip casting. However, under these conditions, thick electrical double layers give a positive contribution to diminish settling and, at the same time, promote particle rearrangement during the deposition stage. Particles in these conditions can pack in an ordered way, due to the repulsive forces existing between them and the consolidated wall. The low deposition rate also enables each particle to search for energetically favorable positions. Therefore, the green density of the slip cast bodies is expected to increase with the zeta potential at low solid loading. In fact, for the 30 and 40 vol% loaded suspensions, Table 1 and Fig. 7 show that the green density was higher in the case of Tiron. On the other hand, for short ranged repulsive forces (lower electrostatic contribution to stabilisation), as in the case of Dolapix, the condition of low solid loading and large average distance between suspended particles enable coagulation in a secondary minimum and, consequently, a less ordered array in the consolidated body. However, when suspensions become more crowded, the larger interaction size in the case of Tiron was shown to be a limiting factor for the packing degree which reaches a maximum at 40 vol% and slightly decreases afterwards.

At high solid loading, the thickness of the hydrated layer, including the diffuse part of the electrical double layer around each particle is reduced and the negative effect of the long-ranged

electrostatic interactions appear to be more pronounced. The average interparticle distance in the wet cake (just after demoulding) is shorter than in the earlier situation and, therefore, the shrinkage during drying should decrease. Despite the decreasing tendency to segregation and the reduction in thickness of hydrated layer with increasing solid loading, a closer approach of particles in suspension does not necessarily translate into a more ordered particle packing within the consolidated layer since the deposition rate increases for a given set of experimental conditions. Hence, the searching of one particle for a low energy position is disturbed by the new incoming particles and the time allowed for particle rearrangement insufficient. At the same time, the stabilisation of concentrated suspensions becomes increasingly difficult according to the rheological measurements obtained and confirmed by the findings of other authors.<sup>25</sup> Consequently, a broader pore size distribution within the cake should be expected.

In contrast to the results with Tiron, the green density continuously increases with increasing solid contents in the case of Dolapix. These results strongly suggest that when the average distance between the suspended particles is shortened until the steric forces become active they can lubricate the particle contacts and hinder particle coagulation in the secondary minimum. For a given solids concentration the effective solids volume fraction and the viscosity of the suspensions will be lower, while the attainable green packing densities will be higher than when strong and pure electrostatic stabilised suspensions are used.

The evolution of the interface cake/suspension in this study was detected manually by introducing a fine wire through the central axis of the slip cast bar being formed. The demoulding operation was performed as soon as the casting was considered complete, i.e. when the typical resistance of the consolidated layer was encountered. Consequently, the moment at which the cast bars become solid is always difficult to determine accurately. Any delay in demoulding will result in a less humid body. However, for a given delay, the difference in

**Fig. 7.** Effect of solid loading on density of slip cast bodies prepared from suspensions dispersed with Tiron (■) and Dolapix (◆).

moisture content will be higher when high solid loaded suspensions are used, due to the lower saturation degree of the plaster mould. This factor might also account for the observed decrease in shrinkage with increasing solid loading.

Figure 7 shows a close correlation between the packing density and the CMC values. This correlation may be explained in the following manner: if the particles were spherical, uniform in size, and formed a regular packed structure with a uniform pore size, the CMC should represent the amount of water filling the interstitial pore space when particles come into contact with each other. Unfortunately, real systems do not fulfil these ideal requirements. For particle shapes other than spherical, the particle size distribution, the segregation phenomena at lower solids concentration, the mutual interference of particles during the deposition stage, the stabilisation degree and the stabilising mechanism are determining factors of the porous microstructures. Depending on their relative importance, the resulting pore size distribution will be broader or narrower, as discussed above. The porous structure, in turn, influences the drying–shrinkage behaviour. In fact, large pores containing higher volumes of liquid phase will have a small contribution to the shrinkage (dS) but a significant influence in the weight loss (dH). This results from the capillary tensions which are inversely proportional to the pore radius.<sup>26</sup> Accordingly, the coarser pores will be emptied by the finer ones and the slope of the straight lines corresponding to the first stage of drying (dS/dH) will decrease. On the other hand, when these lines intercept the humidity axis, the moisture content is lower than it might be if the pores have the same size. This could explain why, in the case of Tiron, the CMC continues to slightly decrease for solid contents > 40 vol%, whilst the green density shows a somewhat inverse trend.

The porosity data of the alumina slip cast bodies are also shown in Table 1, whereas Fig. 8(a) and (b) reports the differential intrusion volume of Hg into the pores as a function of mean pore size for samples prepared with Tiron and Dolapix, respectively. As discussed above, the broadening of the pore size distribution should occur for solid contents higher than the ‘critical’ value at which the CMC becomes almost constant. Figure 8 apparently confirm this trend, especially in the case of Tiron [Fig. 8(a)]. However, the porosity data also displays some incongruity namely, between total pore volume and green density. Some porosity measurements were repeated two or three times to test the reproducibility of this characterisation method. It was concluded that the observed differences are within the experimental error. Alternatively, the

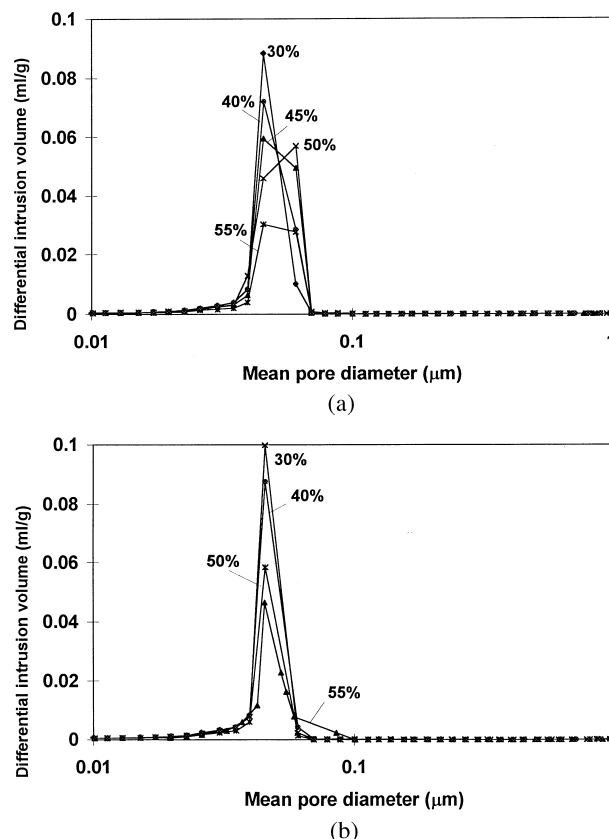


Fig. 8. Incremental intrusion volume curves for the slip cast bodies prepared from suspensions at different solid contents and dispersed with (a) Tiron and (b) Dolapix.

density measurements were consistent. The difference in reproducibility of the measurements performed by these two techniques might derive from the low total pore volume and from different sizes of the samples tested, approximately 8–10 g (density) and 1.5–1.7 g (porosimetry).

The results presented in this work indicate some limitations of the Hg porosimetry method to characterise relatively dense slip cast bodies. Alternatively, drying–shrinkage behaviour revealed to be a very simple and powerful tool to characterise these porous structures. One can also derive further information about the wet microstructure and its dependence upon the relevant factors cited above. Also good correlations may be established between the green microstructure, the rheology of the suspensions and the particle interaction forces.

#### 4 Conclusion

This study has revealed that the stabilising mechanism influences the effective solids volume fraction of the suspended particles and hence, the rheology of the suspensions and the packing behaviour during the slip casting process. At low solid loading high zeta potentials promoted the formation of more regular and ordered

microstructures, and the steric hindrance did not play any important role. When the solid loading increased, the green density obtained from electrostatically stabilised systems using Tiron (a low  $M_w$  sulphonic acid) as dispersant, tended to increase, owing to a reduction of the segregation phenomena, until a maximum was reached. This was followed by a slight decrease because of mutual interferences of particles during deposition. Dolapix (a polyacrylic acid) revealed to be less effective in promoting close particle packing at low solid loading due to its smaller electrostatic contribution to the stabilisation. However, for high solids contents where the interparticle distances were shorter and steric forces became active, Dolapix enabled lower viscosity slurries and higher green packing densities to be obtained.

All the processing variables were reflected in the drying-shrinkage behaviour. The total shrinkage always diminishes with increasing solid loading in suspension. This is mainly due to the thinner hydrated layers surrounding the particles both in the suspension and in the wet body. Any delay in the demoulding operation can accentuate those differences. A close relationship between the CMC and the packing density was observed. The slopes of the straight lines of the Bigot's curves ( $dS/dH$ ) corresponding to the first stage of the drying depend upon the pore size distribution which also affects the CMC values.

Overall, Bigot's curves revealed to be a very simple and powerful tool to characterise the structure of slip cast bodies. It also enables good correlations to be established between the green microstructure, the rheology of the suspensions and the particle interaction forces. In contrast, the evaluation of the pore size distribution in relatively dense slip cast bodies by Hg-porosimetry was found to be a less reliable method.

## Acknowledgements

This work was supported by the European Community, contract CHRX-CT94-0574 in the frame of the Human Capital and Mobility programme and by the JNICT Project no. PBIC/C/CTM/1968/95. We wish to thank both entities for their financial support.

## References

1. Pugh, R. J. and Bergstrom, L., *Surface and Colloid Chemistry in Advanced Ceramic Processing*, Vol. 51, Surfactant science series, Marcel Dekker, New York, 1994.
2. Hunter, R. J., *Foundations of Colloid Science*, Vol. 1, Oxford University Press, 1995.
3. Heimez, P. C., *Principles of Colloid and Surface Chemistry*, 2nd edn, Marcel Dekker, New York, 1986.
4. Israelachvili, J. N., Measurements of hydration forces between macroscopic surfaces. *Chemica Scripta*, 1985, **25**, 7–14.
5. Tonck, A., Georges, J. M. and Loubet, J. L., Measurements of the intermolecular forces and rheology of dodecan between alumina surfaces. *J. Coll. Interf. Sci.*, 1988, **126**, 151–163.
6. Pashley, R. M. and Israelachvili, J. N., DLVO and hydration forces between mica surfaces in  $Mg^{2+}$ ,  $Ca^{2+}$ ,  $Sr^{2+}$ , and  $Ba^{2+}$  chloride solutions. *J. Coll. Interf. Sci.*, 1984, **97**, 446–455.
7. Luckham, P. F., The measurement of interparticle forces. *Powder Techn.*, 1989, **58**, 75–91.
8. Luckham, P. F., Ansarifard, M. A. and de L. Costello, B. A., The relationship between interparticle forces and the bulk rheology of suspensions. *Powder Techn.*, 1991, **65**, 371–379.
9. Adair, J. H., Casey, J. A., Randall, C. A. and Venigalla, S. *Science and Applications of Colloidal Suspensions*, Ceramic Transactions, Vol 54. American Ceramic Society, Westernville, USA, 1995.
10. Lee, W. E. and Rainforth, W. M., *Ceramic Microstructure—Property Control by Processing*, ed. Chapman & Hall, London, 1994.
11. Horn, R. G., Surface forces and their action in ceramic materials. *J. Am. Ceram. Soc.*, 1990, **73**, 1117–1115.
12. Verwey, E. J. W. and Overbeek, J. T. G. *Theory of the Stability of Lyophobic Colloids*, Elsevier Science, Amsterdam, 1948.
13. Hayashi, T., *Surface Chemistry of Ceramic Shaping Processes*. Annual Report for Overseas Readers, Japan Fine Ceramics Association, 1991.
14. Conway, B. E. and Bobry-Duclaux, A., *Rheology—Theory and Applications*, Vol. 3, ed. F. R. Zirich. Academic Press, New York, 1960.
15. Diz, H. H. M., O Estado de Agregação das Partículas de Caulinite e a sua Influência nas Propriedades Reológicas, de Compressão e de Enchimento de Suspensões Argilosas. Ph.D. thesis, University of Aveiro, Portugal, 1984.
16. Tari, G., Ferreira, J. M. F. and Lyckfeldt, O., Influence of magnesia on colloidal processing of alumina. *J. Europ. Cer. Soc.* in press.
17. Graule, Th., Hidber, P. C., Hofmann, H. and Gauckler, L. J., Stabilisation of alumina dispersions with carboxylic acids. *Proceedings of the 2nd Euro Ceramics*, Vol. 1. Aushburg, 1991, pp. 299–305.
18. Graule, Th. and Gauckler, L. J., Electrostatic stabilisation of aqueous alumina suspension by substituted phenols. *3rd Euro Ceramics*, Vol. 1. Madrid, 1993, 491–500.
19. Hunter, R. J., *Zeta Potential in Colloid Science*. Plenum Press, New York, 1982.
20. Higashitani, K., Kondo, M. and Hatade, S., Effect of particle size on coagulation rate of ultrafine colloidal particles. *J. Coll. Interf. Sci.*, 1991, **142**(1), 204–213.
21. Ayral, A. and Phalippou, J., Effect of pH on the rheological properties of a silica hydrosol. *J. Europ. Ceram. Soc.*, 1990, **6**, 179–186.
22. Mooney, M., The viscosity of a concentrate suspension of spherical particles. *J. Coll. Interf. Sci.*, 1951, **6**, 162–170.
23. Sacks, M. D., Properties of silica suspensions and cast bodies. *Am. Ceram. Soc. Bull.*, 1984, **63**, 1510–1515.
24. Reed, J. S., *Introduction to the Principles of Ceramic Processing*. John Wiley & Sons, New York, 1988.
25. Velamakanni, B. V. and Lange, F. F., Effect of interparticle potentials and sedimentation on particle packing density of bimodal particle size distributions during pressure filtration. *J. Am. Ceram. Soc.*, 1991, **74**(1), 166–172.
26. Scherer, G. W., Theory of drying. *J. Am. Ceram. Soc.*, 1990, **73**(1), 3–14.